ℓ_1 controller design for a high-order 5-pool irrigation canal system

Pierre-Olivier Malaterre[1] , Mustafa Khammash[2]

Keywords: control of irrigation canals, civil structures, ℓ_1 control, robustness, integrator, high-order systems, numerical tools

Abstract

The aim of this work is to present an application of recent methods for solving the ℓ_1 design problem, based on the Scaled-Q approach, on a high-order, non-minimum phase system. We start by describing the system which is an open-channel hydraulic system (e.g.: an irrigation canal). From the linearization and discretization of the set of two partial-derivative equations, a state-space model of the system is generated. This model is a high-order MIMO system (five external perturbations w, five control inputs u, five controlled outputs z', five measured outputs y, 65 states x) and is non-minimum phase. A controller is then designed by minimizing the ℓ_1 norm of the impulse response of the transfer matrix between the perturbation w and the output $z = \begin{bmatrix} z' \\ z'' \end{bmatrix}$, where the five additional variable z'' are defined as $z'' = D_u u$. Considering this additional transfer (w to z'') in the minimization problem leads to a better posed problem and provides much better robustness margins. Time-domain template constraints are added in order to force integrators into the controller. The numerical resolution of the problem proved to be efficient, despite of the characteristics of the system. The obtained results are compared in the time-domain to classical PID and LQG controllers, both on linear and non-linear simulated plants. The results proved to be very good in terms of performance and robustness, in particular for the rejection of the worst-case perturbation.

[1] Visiting Scientist at Iowa State University from May 1999 to August 2000, Research-Engineer at UR Irrigation, Cemagref, 361 rue J.-F. Breton, BP 5095, 34033 Montpellier Cedex 1, France, pom@montpellier.cemagref.fr

[2] Department of Electrical and Computer Engineering, Control Group, Coover Hall, Iowa State University, Ames, Iowa 50011-3060, khammash@iastate.edu, acknowledges support by NSF grant ECS 9457485

1 Introduction

An irrigation canal is an open-channel hydraulic system whose main objective is to convey water from a source (dam, river) to users (agricultural lands, but also industries and cities). Such systems can be very large (several hundreds of kilometers), and different objectives are assigned to their managers. The main general one is to provide water to the different users at the good moment and in the good quantity, and to guarantee the safety of the infrastructure. In particular, a major concern is to prevent the canals from overtopping, but also from having water levels inside the pools below the supply depths of the offtakes. The cross-structures used as actuators also have maximum allowed gate openings. These constraints are typically time-domain constraints on the bound (ℓ_∞ norm) of some controlled signals z. On the other side, a bound on the perturbation w is also known (e.g.: subscribed maximum discharge at offtakes), which is also an information on its ℓ_∞ norm. This justifies the idea to design a controller by minimizing the ℓ_1 norm of the impulse response of the considered transfer matrix $\Phi : w \to z$, since this norm is the induced ℓ_∞-ℓ_∞ norm ([1]).

Most of the technics that have been used so far, for the automation of irrigation canals, are based on PID, Internal Model and Fuzzy Control. Several works on Predictive Control, LQG or $\mathcal{H}_\infty$ design methods will certainly have applications in the near future ([2]).

To our knowledge, this is also the first time a ℓ_1 controller is designed on such a large system. In the past, the main constraint was the lack of good numerical tools to solve the corresponding minimization problem. The work presented in this paper could be carried out thanks to recent advances on this matter ([3]).

2 Description of the System

2.1 Considered canal example and objectives

The system considered in this paper is the canal "type 1" from the Cemagref Bench Mark canals ([4]). These canals have been defined from two dimensionless coefficients, in order to cover all kinds of hydraulic behaviors. Canal "type 1" corresponds to a short pools canal, with an almost first-order flow dynamics and with slowly

damped wave oscillations. It is a 15 km long canal, composed of five identical pools (3000 m long each) separated by gated cross structures (Figure 1). The cross section is trapezoidal, with a bed width of 7 m and a side slope of 1.5. The longitudinal slope of the canal is 1.10^{-4}, with an additional 0.04 m drop at each structure. The nominal flow in the canal is around 7 m^3/s.

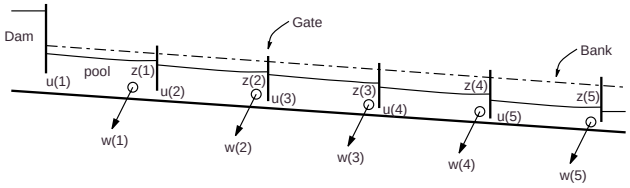

Figure 1: Canal "type 1" from Cemagref Bench Marks

The gate opening u located upstream of each pool is the control action variable ($u_{i=1,...,5}$). An offtake is located downstream of each pool, 5 m upstream of the next gate. These offtakes can withdraw water from the main canal to supply their corresponding users. This flow is the external perturbation w acting on the system ($w_{i=1,...,5}$). In this example, the control objective is to maintain each water level z' downstream of each pool ($z'_{i=1,...,5}$) as close as possible to its target, and in particular in a given range $[z'_{min}, z'_{max}]$ in order to prevent any overtopping or insufficient hydraulic head at the offtake. These water levels are also the measured variables ($y_{i=1,...,5}$) provided to the controller K to be designed.

An additional transfer (w to $z'' = D_u u$, where D_u is a 5×5 matrix) is also considered in the minimization problem in order to get good robustness margins. The total controlled variable z is therefore defined as $z = \begin{bmatrix} z' \\ z'' \end{bmatrix}$. By doing that we change the previous one-block problem to a two-block column problem (see [1] p. 127).

A time-domain template is added into the minimization problem, in order to constraint the controller to have integrators in the transfers $w \rightarrow z'$. This, in turn, guarantees zero steady-state errors.

This template is given as $a_{ij}(k) \leq \Sigma_{l=0}^{k} \Phi(l)_{ij} \leq b_{ij}(k)$ (Φ is defined in section 2.3) with, for $i = 1..5$, $j = 1..5$: $a_{ij}(k) = -b_{ij}(k) = -1$ for $k < N$ and $a(k) = b(k) = 0$ for $k \geq N$ (N=50 in our example). No template is added on Φ_{ij}, for $i = 6..10$, $j = 1..5$, since they correspond to the transfers $w \rightarrow z''$. Three other options to add an integrator have been tested, but this one proved to be the best in terms of robustness margins, order of the controller and speed of the convergence of the upper and lower bounds of the Scaled-Q approach.

2.2 Equations

The dynamic behavior of water in an open-channel is well described by the so-called Saint-Venant's equations:

$$\begin{cases} \frac{\partial Q}{\partial x} + \frac{\partial S}{\partial t} = 0 \\ \frac{\partial Q}{\partial t} + \frac{\partial \frac{Q^2}{S}}{\partial t} + g.S\frac{\partial Z}{\partial t} + g.S.J = 0 \end{cases} \quad (1)$$

where Q is the discharge (m^3/s), S the wetted cross-area (m^2), Z the water elevation (m), J the friction slope, x the longitudinal abscissa (m) and t the time (s). The friction slope J is usually obtained from the Manning-Strickler formula: $J = \frac{n^2 Q^2}{S^2 R^{\frac{4}{3}}}$, where n is the Manning's coefficient (0.02) and R is the hydraulic radius (m) ($R = \frac{S}{P}$, where P is the wetted perimeter).

The equation of the flow through the gate structure is usually taken as:

$$Q = C_d \sqrt{2g} L u \sqrt{z_{up} - z_{dn}}$$

where C_d is the gate discharge coefficient (0.82), L the gate width (10.18 m), u the gate opening (m) and z_{up} (resp. z_{dn}) the water level upstream (resp. downstream) of the gate (m).

The two hyperbolic, first-order, non-linear, partial-derivative equations (1) are linearized and discretized in time (Δt time step) and space (Δx space step) through the implicit Preissmann finite difference scheme. The gate structure equation is linearized and introduced at the proper locations in the scheme. This leads to a discrete-time state-space representation ([5]):

$$\begin{cases} x^+ = Ax + Bu + B_w w \\ y = Cx \\ z' = Dx \\ z'' = D_u u \end{cases} \quad (2)$$

where A, B, B_w, C, D and D_u are real constant matrices of appropriate dimensions. This system is stable but non-minimum phase. The modulus of the maximum eigenvalue is 0.983 and the modulus of the maximum transmission zero is 3.78 (discrete time in z-transform).

2.3 Problem Setup

As justified in the Introduction section, our objective is to find a stabilizing linear time-invariant (LTI) discrete-time controller K which minimizes the ℓ_1 norm of the impulse response of the transfer matrix $\Phi : w \rightarrow z$. This can be stated as solving:

$$\gamma^{opt} = \inf_{\text{K stabilizing}} \|F_l(P, K)\|_1 \quad (3)$$

where P represents the LTI discrete-time generalized plant, K the LTI discrete-time controller, $F_l(P, K) = \Phi$

the lower linear fractional transformation of P by K. We assume the dimensions of w, z, u, and y are n_w, n_z, n_u, and n_y respectively. It can be shown (see [1] for example), that this problem can be formulated as that of finding:

$$\gamma^{opt} = \inf_{Q \in \ell_1^{n_u \times n_y}} \|H - U * Q * V\|_1 \tag{4}$$

where $*$ denotes convolution, $H \in \ell_1^{n_z \times n_w}$, $U \in \ell_1^{n_z \times n_u}$, and $V \in \ell_1^{n_y \times n_w}$ are fixed and depend on the problem data: P, n_w, n_z, n_u, and n_y.

3 Scaled-Q method

3.1 Theoretical Principles

In [3] it is proved that upper and lower bounds for γ^{opt} can be obtained by solving the two following finite linear programs:

A lower bound for γ^{opt}:

$$\underline{\nu}_N(\beta) = \min_{Q \in \ell_1^{n_u \times n_y}} \|H - R\|_1$$
$$\text{subject to } \begin{cases} \|Q\|_1 \leq \beta \\ P_N R = P_N(U * Q * V) \end{cases} \tag{5}$$

where P_N is the truncation operator and β sufficiently large.

An upper bound for γ^{opt}:

$$\overline{\nu}_N(\beta) = \min_{Q \in \ell_1^{n_u \times n_y}} \|H - R\|_1$$
$$\text{subject to } \begin{cases} \|Q\|_1 \leq \beta \\ R = U * P_N(Q) * V \end{cases} \tag{6}$$

In [3] it is proved that when an optimal solution $Q_{opt} \in \ell_1^{n_u \times n_y}$ for the ℓ_1 problem (equ. (4)) exists (in particular it is the case when $\hat{U}$ and $\hat{V}$ have no zeros on the unit circle), then $\underline{\nu}_N(\beta) \nearrow \gamma^{opt}$, $\overline{\nu}_N(\beta) \searrow \gamma^{opt}$ and $Q_N \to Q_{opt}$ as $N \to \infty$. This result holds true with the additional template constraints ([6]).

3.2 Numerical Approach

The first step of the numerical resolution is to get a Youla parametrization of all stabilizing controllers. Given the state-space representation of a generalized plant P, three stable systems H, U, and V are generated such that the Q-parametrizaton of the closed-loop transfer function Φ is given by $H - U * Q * V$. The stabilizing state-feedback and filter-gain matrices for the observer-based central stabilizing controller for this Youla parametrization can be obtained through pole placement. But on high-order system this direct approach does not always give good results. We obtained better results by using a LQG design. In fact, this step is quite important since the maximum eigenvalues of the H, U and V transfer matrices will determine the length of their Finite Impulse Response (FIR) approximations.

The second step is to translate all equations and constraints of the above problems (equ. (5) and (6)) into a classical finite dimension linear programing problem:

$$\min_x f'x \text{ , subject to } \begin{cases} A_1 x \leq b_1 \\ A_2 x = b_2 \end{cases} \tag{7}$$

In our example the number of variables (resp. constraints and non-zero coefficients) reached 7551 (resp. 6765 and 2246110) for the upper bound and 2451 (resp. 1665 and 283960) for the lower bound, for length(Q)=16. The linear programming problem was solved using $Cplex$© 6.6.

Then a state-space realization of the optimal controller K is obtained, given the state-space realization of the plant P and an impulse response of the optimal Youla parameter Q obtained as output of the above linear program. This controller K is obtained from the solution of the upper bound problem. The solution of the lower bound problem is just used to give an indication on how far the current finite support solution is from the optimal one.

4 Results

In this section the ℓ_1 controller is tested and compared to classical PID and LQG controllers. These reference PID and LQG controllers are designed as explained in [7], [8] (for PID) and [5] (for LQG). This comparison is not made in order to prove than one controller is better than another, but to show what type of performance the ℓ_1 controller can achieve compared to typical controllers that exist for this type of system. This comparison will be made on different aspects: closed-loop norms (ℓ_1, $\mathcal{H}_2$ and $\mathcal{H}_\infty$), order of the controller, rejection of some worst-case perturbations, rejection of classical periodic perturbations, and robustness margins.

4.1 Norms

We verify that when the parameter length(Q) is increased (from 1 to 16 in Figure 2), the lower and upper bound of the Scaled-Q method converge. The improvement of the ℓ_1 norm is important since it is decreased,

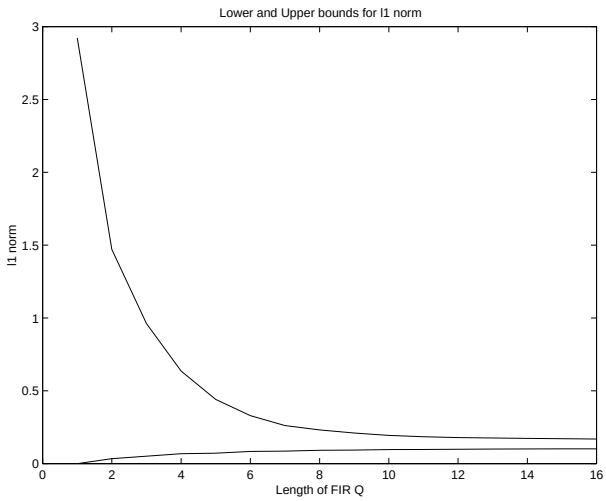

Figure 2: lower and upper bounds of $\|\phi\|_1$

	$\Phi_{K=0}$	Φ_{PID}	Φ_{LQG}	Φ_{ℓ_1}
ℓ_1 norm	0.623	0.369	0.274	0.17
$\mathcal{H}_2$ norm	0.102	0.111	0.095	0.139
$\mathcal{H}_\infty$ norm	0.495	0.155	0.118	0.135
order	0	5	75	137

Table 1: Norms and orders of the controllers

for the upper bound, from 2.92 to 0.17. Further improvement can be obtained by increasing length(Q), but at the cost of larger linear programs to solve, and probably higher order controllers.

In Table 1 are displayed the ℓ_1, $\mathcal{H}_2$ and $\mathcal{H}_\infty$ norms of the open-loop map (K=0) and closed-loop maps for the three controllers. The order of the controller is also indicated. As expected, the ℓ_1 controller provides the smallest ℓ_1 norm (0.17). The $\mathcal{H}_2$ norm of the ℓ_1 controller is larger than those of the PID and LQG controllers, but the increase is small compared to the improvement in ℓ_1 norm. The cost to pay for that is an increase of the order of the controller (137 instead of 75 for LQG and 5 for PID). It is possible to select a suboptimal solution obtained for a smaller value of length(Q). For example, for length(Q)=10 we have a ℓ_1 norm of 0.19 for a 109 order controller.

4.2 Worst-Case Perturbation

In this section the ℓ_1 controller is tested on worst-case perturbations and compared to the PID and LQG controllers.

Since the ℓ_1 norm is defined as $\|\Phi\|_1 = \sup_{\substack{w\in\ell_\infty \\ w\neq 0}} \frac{\|\Phi * w\|_\infty}{\|w\|_\infty}$, it is easy to show that the worst-case perturbation w_0 such that $\|\Phi\|_1 = \frac{\|\Phi * w_0\|_\infty}{\|w_0\|_\infty}$ is obtained by the following procedure:

if $\Phi = \{\phi_{ij}\}_{\substack{i=1,\ldots,nz \\ j=1,\ldots,nw}}$ and i_0 is the row such that $\|\Phi\|_1 = \sum_{j=1}^{nw} \|\phi_{i_0 j}\|_1$ then, for a given t, w_0 is defined by: $(w_0)_j(k) = sign(\phi_{i_0 j}(t-k))$, for $j = 1,\ldots,nw$ and for $0 \leq k \leq t$. We have $\|w_0\|_\infty = 1$ and for t sufficiently large, we get $\|\Phi * w_0\|_\infty$ arbitrary close to $\|\Phi\|_1$.

In fact, instead of using the $sign$ function defined as ($sign(x) = +1$ if $x \geq 0$ and $sign(x) = -1$ if $x < 0$) we used the $sign_\epsilon$ function defined as ($sign_\epsilon(x) = +1$ if $x > \epsilon$, $sign_\epsilon(x) = -1$ if $x < -\epsilon$ and $sign_\epsilon(x) = 0$ if $-\epsilon \leq x \leq \epsilon$). The advantage of using such function is to get a much more realistic ϵ-worst-case perturbation w_ϵ, with much less switches between -1 and $+1$, especially when the impulse response of Φ is oscillating around 0. By selecting ϵ close to 0, we can get a corresponding norm $\|\Phi * w_\epsilon\|_\infty$ as close to the worst one as desired.

The ℓ_1, PID and LQG controllers have been tested and compared on the ϵ-worst-case perturbation calculated for the LQG controller (noted $w_{\epsilon,LQG}$). The ℓ_1 norm of this LQG controller (which is different from the one used as the central controller for the Youla parametrization) is 0.27. The $w_{\epsilon,LQG}$ perturbation calculated for $\epsilon = 1.10^{-3}$ gives $\|\Phi_{LQG} * w_{\epsilon,LQG}\|_\infty = 0.24$, where Φ_{LQG} is Φ calculated with the LQG controller. For the same perturbation $w_{\epsilon,LQG}$, the ℓ_1 controller gives $\|\Phi_{\ell_1} * w_{\epsilon,LQG}\|_\infty = 0.152$ which proves a significant improvement compared to the LQG controller (-37%).

The same comparison was carried out on a full non-linear simulation model (SIC© software [9]) and even though the peaks $\|z\|_\infty$ obtained by both ℓ_1 and LQG controllers were smaller (Figure 3), the relative improvement (-37%) was the same (0.095 for the ℓ_1 controller instead of 0.15 for the LQG controller). The results obtained by the PID controller are much worse, probably due to smaller robustness to non-linearities (Table 2).

We also checked all three controllers on the ϵ-worst-case perturbation w_{ϵ,l_1} (resp. $w_{\epsilon,PID}$) calculated for the ℓ_1 (resp. PID) controller. The ℓ_1 controller was always giving the best results in terms of peak $\|z\|_\infty$ with also usually less control efforts u than with the LQG and PID controllers.

4.3 Classical Periodic Perturbation

In this section the ℓ_1 controller is tested on a classical periodic perturbation and compared to the PID and LQG controllers. This classical periodic perturbation was obtained from real measurements on an irrigation canal (from Société du Canal de Provence, Aix-en-Provence, France). It can be observed on large canals, when no unusual events occur (rain, closure of

function	$K=0$	PID	LQG	ℓ_1
$\|S_o\|_\infty$	1.0	5.81	4.70	3.04
$\|T_o\|_\infty$	0.0	5.17	4.58	2.43
$\|S_i\|_\infty$	1.0	28.74	2.65	8.98
$\|T_i\|_\infty$	0.0	28.68	1.95	8.71
$\|S_i.K\|_\infty$	0.0	24.10	4.12	6.32
$\|S_o.G\|_\infty$	18.64	6.06	3.06	3.91

Table 2: Robustness margins

secondary canals, breakdowns, etc.).

On this type of perturbation, which is very different from the worst case scenario, the ℓ_1 controller is still giving slightly better results than the LQG and PID controllers on both linear and non-linear models (Figure 4).

4.4 Robustness Margins

The robustness characteristics of the ℓ_1 controller are good and comparable to the ones of the LQG controller (Table 2). The output sensitivity function S_o and the output complementary sensitivity function T_o are better for the ℓ_1 controller, while the input sensitivity function S_i, the input complementary sensitivity function T_i, the input sensitivity function times the controller $S_i.K$ and the output sensitivity function times the model $S_o.G$ are better for the LQG controller. Margins of the PID controller are much smaller, which explains the degradation of the results on the non-linear simulation model (Figure 3).

5 Conclusion

The results presented in this paper show that the theoretical approach and numerical tools used to solve the ℓ_1 controller design problem proved to be efficient and numerically reliable. Due to the size of the system, and its characteristics in terms of zeros, this was not an obvious statement. The results obtained in terms of reduction of the ℓ_1 norm of the closed-loop map $\Phi : w \to z$ also proved to be very important, compared to classical PID and LQG controllers. This was confirmed by time-domain simulations of the rejection of worst-case perturbations, on both a linear and a non-linear simulation model. On a practical point of view, this improvement is useful due to the interpretation of the ℓ_1 norm as the induced $\ell_\infty - \ell_\infty$ norm. It should have an impact on an increased safety of the infrastructure and potentially on the reduction of civil engineering costs.

The algorithms used can still and will be improved in the future. In particular, instead of considering FIR approximations of the U and V transfer matrices, it may be more efficient to look for a polynomial factorization of these terms. This will allow to consider longer length(Q), larger systems, or more constraints on the Φ transfer matrix.

Acknowledgment

The results of this paper were obtained during my stay at ISU as a Visiting Scientist. I would like to express deep gratitude to Mustafa Khammash who kindly welcomed me in his research group. I would also like to thank Cemagref, Montpellier, France for its financial support and my colleagues there that accepted to do part of my share of work during this period.

References

[1] M. A. Dahleh and I. J. Diaz-Bobillo, *Control of uncertain systems: a linear programming approach*. Prentice-Hall, 1995.

[2] P.-O. Malaterre, D. C. Rogers, and J. Schuurmans, "Classification of canal control algorithms," *ASCE Journal of Irrigation and Drainage Engineering*, vol. 124, pp. 3–10, January/February 1998. ISSN 0733-9437.

[3] M. Khammash, "A new approach to the solution of the ℓ_1 control problem: the Scaled-Q method," *IEEE Transaction on Automatic Control*, vol. 45, pp. 180–187, February 2000.

[4] J.-P. Baume, J. Sau, and P.-O. Malaterre, "Modeling of irrigation channel dynamics for controller design," *IEEE International Conference on Systems, Man and Cybernetics (SMC98), San Diego, California*, pp. 3856–3861, October 11 to 14 1998.

[5] P.-O. Malaterre, "Pilote: linear quadratic optimal controller for irrigation canals," *ASCE Journal of Irrigation and Drainage Engineering*, vol. 124, pp. 187–194, July/August 1998. ISSN 0733-9437.

[6] X. Qi, M. H. Khammash, and M. V. Salapaka, "Optimal controller synthesis with multiple objectives," *ACC*, 2001. submitted.

[7] P.-O. Malaterre and J.-P. Baume, "Optimum choice of control action variables and linked algorithms. comparison of different alternatives," *Workshop on Modernization of Irrigation Water Delivery Systems, in Phoenix, Arizona, USA*, October 18-21 1999.

[8] J.-P. Baume, P.-O. Malaterre, and J. Sau, "Tuning of PI to control an irrigation canal using optimization tools," *Workshop on Modernization of Irrigation Water Delivery Systems, in Phoenix, Arizona, USA*, October 18-21 1999.

[9] P.-O. Malaterre and J.-P. Baume, "Sic 3.0, a simulation model for canal automation design," *International Workshop on the Regulation of Irrigation Canals: State of the Art of Research and Applications, RIC97, Marrakech (Morocco)*, April 22-24 1997.

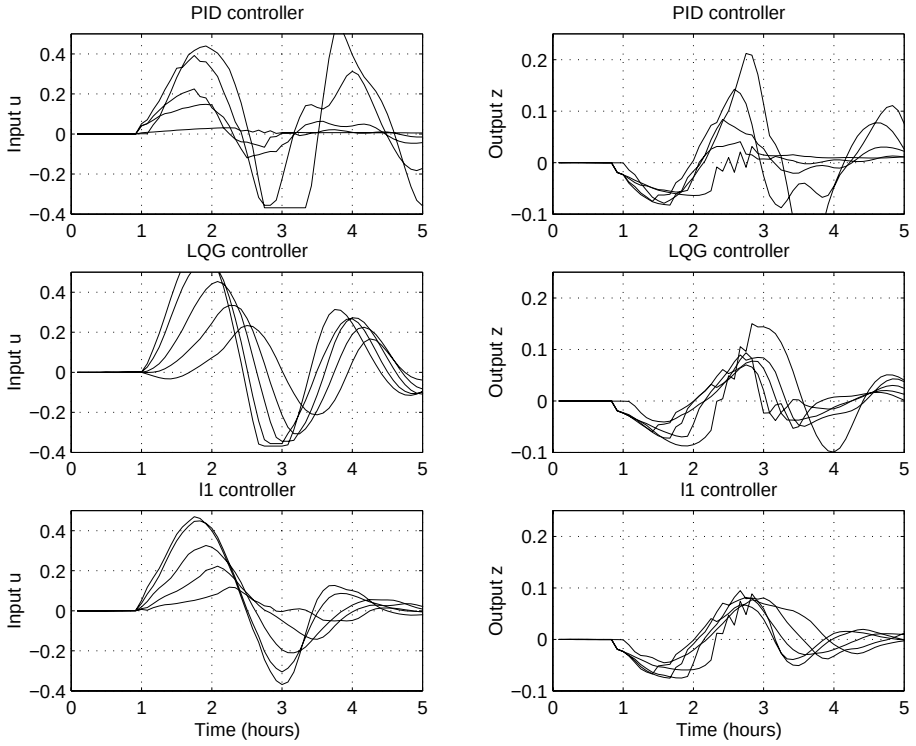

Figure 3: Comparison of controllers on $SIC^{©}$ (non-linear model) on ϵ-worst-case perturbation $w_{\epsilon,LQG}$ for LQG controller

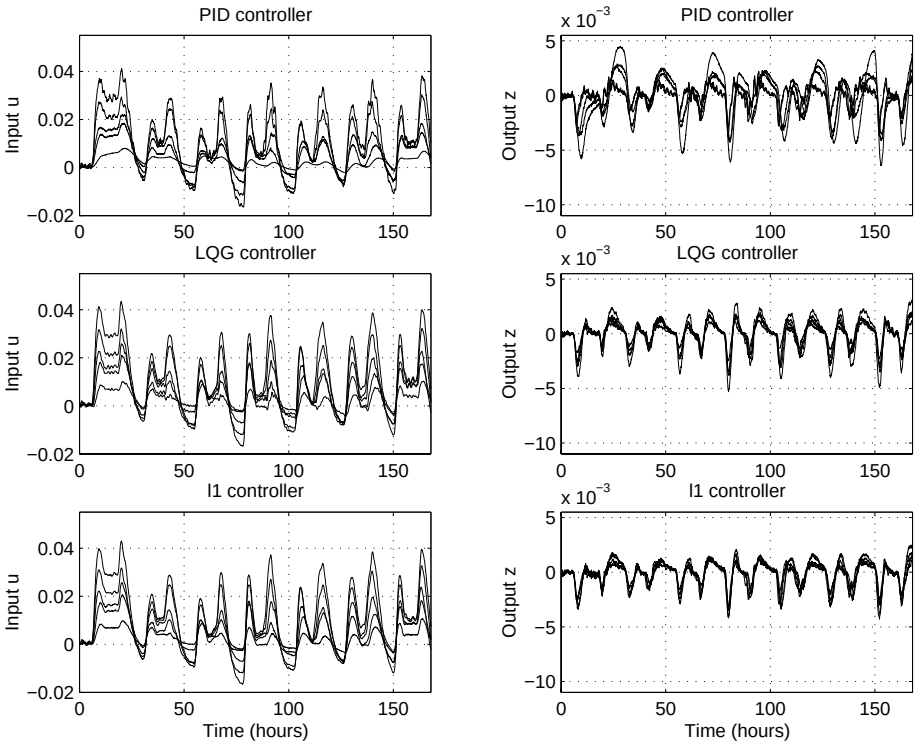

Figure 4: Comparison of controllers on $SIC^{©}$ (non-linear model) on classical periodic perturbation